UDK   622.785; 546.824
Reheating of Zinc-titanate Sintered Specimens

N. Labus,[1*)], S. Mentus[2,3], S. Rakić[4], Z. Z. Đurić[1], J. Vujančević[1], M.V. Nikolić[5]

[1]Institute of Technical Sciences of SASA, Knez Mihailova 35, 11000 Beograd, Serbia
[2]Faculty of Physical Chemistry, Studenski trg 12-16, 11158 Belgrade, University of Belgrade, Serbia
[3]Serbian Academy of Sciences and Arts, Knez Mihailova 35, 11000 Belgrade, Serbia
[4]Institute of Physics, Faculty of Natural Sciences, University of Novi Sad, Trg D. Obradovica 6, 21000 Novi Sad, Serbia
[5]Institute for Multidisciplinary Research, University of Belgrade, Kneza Viseslava 1, 11000 Beograd, Serbia

Abstract:
The scope of this work was observing dimensional and heat transfer changes in $ZnTiO_3$ samples during heating in nitrogen and air atmosphere. Interactions of bulk specimens with gaseous surrounding induce microstructure changes during heating. Sintered $ZnTiO_3$ nanopowder samples were submitted to subsequent heating. Dilatation curves and thermogravimetric with simultaneous differential thermal analysis TGA/DTA curves were recorded. Reheating was performed in air and nitrogen atmospheres. Reheated samples obtained at different characteristic temperatures in air were analyzed by X-ray diffraction (XRD). Microstructures obtained by scanning electron microscopy (SEM) of reheated sintered samples are presented and compared. Reheating in a different atmosphere induced different microstructures. The goal was indicating possible causes leading to the microstructure changes.
Keywords: Dilatometry, Sintering.

1. Introduction

In the zinc oxide titanium oxide binary system phase transformations encountered during heating are present in the following sequence [1]. The first is a low temperature cubic phase - $Zn_2Ti_3O_8$ that slowly transforms from 600^oC to 765^oC with heat emission to a hexagonal $ZnTiO_3$ metastable perovskite phase. Metastability of this phase originates from the cation ratio that is a tilting highly distorted structure [2,3]. The second, $ZnTiO_3$ with a narrow temperature stability interval ends in an energy consuming fast phase transition to the Zn_2TiO_4 spinel phase in the 965^oC to 1010^oC temperature interval [4]. Actually, two distinct phases emerge after this phase transition, the most stable Zn_2TiO_4 spinel phase and TiO_2 rutile [5].

If gas is introduced in the heating chamber and atmospheric pressure maintained, heating experiments are referred to as conducted in a specified different atmosphere. Air atmosphere is most frequently used. Other gases are introduced in the closed chamber where

_____

*) **Corresponding author**: nebojsa.labus@itn.sanu.ac.rs

_____

the sample is positioned as purged, which stands for regulated flow of the chosen gas. Powders and polycrystalline bulk samples respond differently to atmosphere changes, especially in the case of oxides and air. Powders compacted from small particles exposed to a certain atmosphere interact through a highly developed surface area [6], while polycrystalline bulk materials interact mainly through high diffusion paths [7] such as grain boundaries and also through grain surfaces on the bulk planes exposed to the atmosphere [8]. The atmosphere during thermal treatment influences the non-stoichiometric metal oxide equilibrium that results in property changes [9,10]. In the case of material transport enabled by point defects, the pressure of the gas expected to change the stoichiometry in the metal oxide experimentally can be set up as continuously changing in a large scale of values. Then the induced responding change in the observed property will hopefully make a detectable and recognizable quantity shift. That change can be afterwards attributed to certain point defect species and the corresponding model of the material transport by diffusion [11,12].

Dilatation of a specimen can be observed during sintering where a powder compact changes into a polycrystalline specimen [13]. During reheating the sample exhibits a specific coefficient of thermal expansion. Differential thermal analysis observes the same events using heat transfer. If the atmosphere influence is connected to a particular diffusion process either by promoting it or inhibiting it, the overall change must be detected by both techniques. In such a manner, we have observed the same characteristic events in their intensity as well as in energy consumption. This can lead to a better understanding of the observed material properties in different conditions.

2. Experimental

Zinc – titanate nanopowder $ZnTiO_3$ 99.5% [12036-43-0] CAS 634409-100G, with a particle size of 40 nm respectively, was compacted at 100 MPa double sided uniaxially and then sintered in a dilatometric furnace at 900^oC and 1200^oC in air atmosphere with a heating rate of 10°/min. Sintered samples were then reheated in dilatometric furnace in air atmosphere with a heating rate 10^oC/min to temperatures a hundred degrees lower than the sintering temperature, i.e. 800^oC and 1100^oC, with a holding time of 20 minutes. These samples are referred to as the first batch and reheating was named the second run. Second batch samples of compacted $ZnTiO_3$ nanopowder were compacted at 200 MPa and sintered to 900^oC and 1100^oC in a Lenton tubular furnace in air. Reheating was performed in a dilatometer furnace to 900^oC and 1100^oC in air and nitrogen. The heating program schedule for sintering was 10^oC/min up to 900^oC and 1100^oC, isothermal holding 1h, with cooling -25^oC to 400^oC. Reheating, the second run, in different atmospheres at 10°/min heating rate to 1100^oC, holding of 20 minutes and during this second heating dilatation was recorded. The atmospheres used for the second batch, second run heating cycle were air without flow and nitrogen atmosphere with 1.11 cm^3s^{-1} flow. The specimen was cleaned by evacuating the chamber to 60 Pa, and then purging with nitrogen, repeating the procedure twice. Then nitrogen was induced with a regulated flow and the temperature program was started. Dilatation and temperature were recorded. A Bähr GmbH model 802s dilatometer was used.

Thermo gravimetric (TG) and differential thermal analyses (DTA) of powder samples and sintered specimens were done with Pt pans, in the temperature interval from room temperature up to 1200^oC, in both nitrogen and air atmospheres. TGA and DTA were carried out simultaneously using a SDT 2960 thermobalance TA instrument. The heating rate was 15^oC/min, while the gas flow rate was $70cm^3s^{-1}$. No special cleaning procedure was performed and nitrogen flow was induced simultaneously with start of the temperature program.

X ray diffractometry was performed on a Rigaku MiniFlex600 with accelerating voltage U=40kV, current I=15mA with a CuKα cathode, graphite secondary monochromator,

_____

2θ range 10° to 100°, step/holding time $0.02^{o}/4s$. Structural refinement was carried out by the Rietveld method using the GSAS package [14] with the EXPGUI graphical user interface [15].

Scanning electron microscopy was performed on a VEGA TS 5130MM device Vega Tescan Digital Microscopy Imaging with accelerating voltage 20keV. Sintered specimens before reheating were manually polished with SiC papers with grit P400 and P2000 and water as a lubricant. Specimens were then polished with a 1 micron Buehler Metadi II diamond polishing paste. SEM images of second batch reheated samples were recorded on breakage surfaces.

3. Results and discussion

During reheating to 1100°C of $ZnTiO_3$ samples initially sintered at 1200°C, unexpected sudden small dimensional changes were noticed as shown in fig.1. The dimensional changes occurred in the temperature region from 387°C to 581°C. Since the observed dimensional changes were rather small compared to the first heating cycle characteristic for sintering phenomenon, the same dilatation curve was presented on both sides of the dimensional length scales, fig.1. Dimensional changes on both diagrams at 950°C for the annealed and 963°C for the sintered sample correspond to the phase transition temperature declared as perovskite $ZnTiO_3$ to spinel Zn_2TiO_4. A scanning electron micrograph of a polished specimen is shown on the right side in fig.1. The mean grain size was estimated as 2.78 microns [16]. The grain size was increased by about 30% during the reheating process [17].
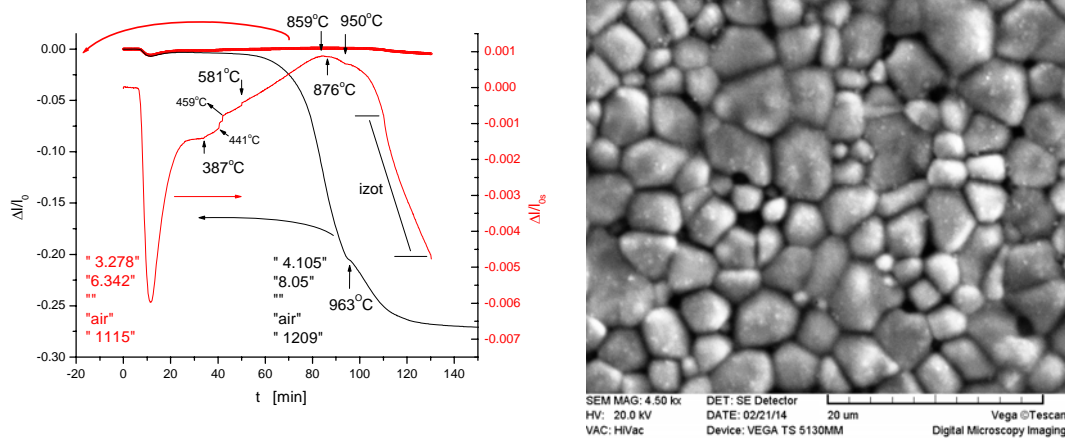

Fig. 1. Dilatograms of $ZnTiO_3$ sample sintered at 1200°C and reheated at 1100°C in the second run, with characteristic values and temperature intervals.

For sintered specimens obtained at 900°C, reheating was performed at a lower temperature of 800°C with isothermal holding for 20 minutes. Dilatograms shown in fig.2 enabled us to notice a pure sintering phenomenon without a phase transition during sintering and thermal expansion with a characteristic temperature at 904°C ascribed to the temperature schedule change from 10°C/min heating rate to isothermal holding and can be explained as equalizing a constant number of oxygen vacancies. The microstructure obtained is presented at the right side of fig.2, and the mean grain size is 0.45 microns. Enlargement compared to sintered grain size was estimated roughly as 30% [17].
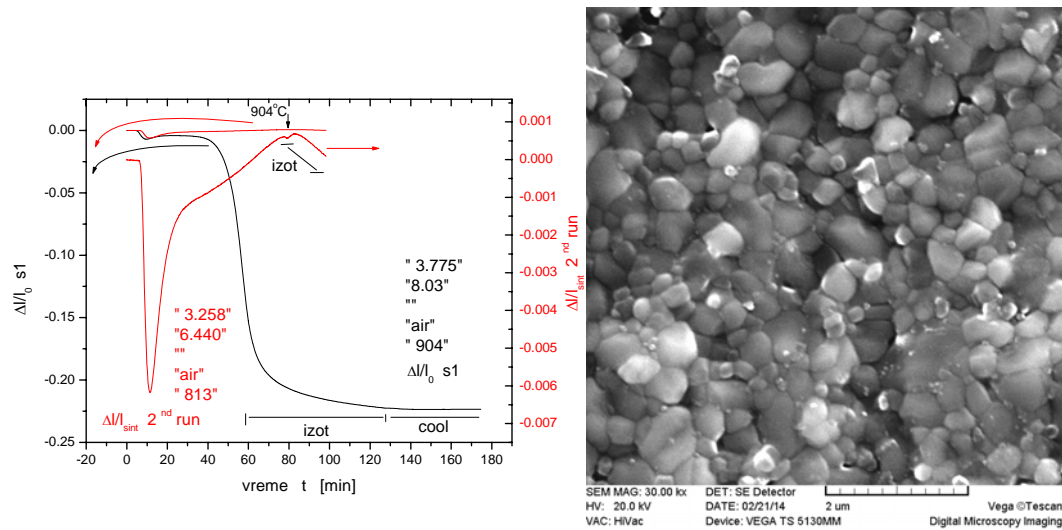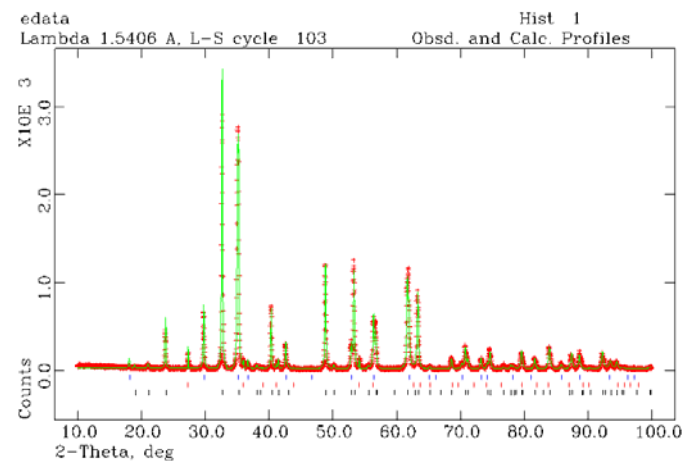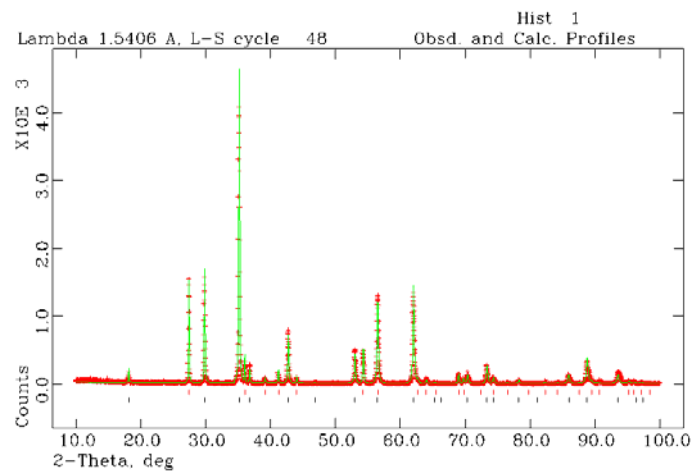
Fig. 2. Dilatograms of $ZnTiO_3$ sample sintered at 900^oC and reheated at 800^oC in the second run, with characteristic values and temperature intervals.

Fig. 3. XRD diffractograms of reheated $ZnTiO_3$ a) first run sintered at 900^oC reheated at 800^oC, first row Zn_2TiO_4 indexed blue, second row TiO_2 rutile indexed red, third row $ZnTiO_3$ indexed black, b) first run sintered at 1200^oC reheated at 1100^oC, first row TiO_2 rutile indexed red, second row Zn_2TiO_4 indexed black.

_____

Tab. I Phase composition, lattice parameters and crystallite size before and after reheating at lower 900°C/800°C and higher 1200°C/1100°C temperatures.

Heating sintering 900°C 10°C/min, 900°C 1h				
phase	$Zn_2Ti_3O_8$	$ZnTiO_3$	Zn_2TiO_4	TiO_2
Composition wt%	1.756%	81.096%	14.343%	2.805%
Unit cell Å	a=8.40648	a=5.0731; c=13.9176	a=8.44931A	a=4.5853; c=2.9562
Reheating 800°C 10°C/min, 800°C 20 min				
phase	$Zn_2Ti_3O_8$	$ZnTiO_3$	Zn_2TiO_4	TiO_2
Composition wt%	/	65.03 wt.%	32.81 wt.%	2.16 wt.%
Unit cell Å	/	a=5.0792(2), c=13.9420(8)	a=8.4670(2)	a=4.6148(3), c=2.9628(4)
Crystallite nm		87 nm	451 nm	

Heating sintering 1200°C 10°C/min, 1200°C 1h		
phase	Zn_2TiO_4	TiO_2
Composition wt%	75.93%	24.7%
Unit cell Å	a=8.4559	a=4.5594; c=2.9592
Reheating 1100°C 10°C/min, 1100°C 20 min		
phase	Zn_2TiO_4	TiO_2
Composition wt%	73.22 wt.%	26.78 wt.%
Unit cell Å	a=8.45852(14)	a=4.5945(2), c=2.9609(2)
	968 nm	262 nm

Diffractograms of samples sintered/reheated 900°C/800°C and 1200°C/1100°C are presented on fig.3. Phases of $ZnTiO_3$ perovskite and Zn_2TiO_4 spinel structure are clearly recognizable and slightly more pronounced compared to the diffractograms of sintered $ZnTiO_3$ nanopowder presented and analyzed before [13]. Samples were analyzed for the presence of $ZnTiO_3$, Zn_2TiO_4, $Zn_2Ti_3O_8$ and r-TiO_2 (rutile). $ZnTiO_3$ was refined as hexagonal, space group $R\bar{3}$ (rhombohedral cell). Starting values were taken from our previous paper and all parameters were varied. Table 1 quantitatively explains the phase compositions. For samples sintered at the lower temperature 900°C/800°C, the Zn_2TiO_4 phase content is almost 15% in the first run, but its content almost doubles after reheating (second run). At the same time the low temperature $Zn_2Ti_3O_8$ phase vanishes.

Small changes in lattice parameters can also be noted after reheating. It should be mentioned that the starting powder had a particle size estimated by nitrogen adsorption to be 30 nm [6]. Dilatograms recorded during sintering at 900°C show an extremely fast sintering process, which explains the large amount of sustained coherent perovskite $ZnTiO_3$ phase. Further heating leads toward stable phases such as orto Zn_2TiO_4 phase that again explains lowering of the lattice parameters [18] since metastability of the perovskite $ZnTiO_3$ phase originates from the tolerance factor and plane tilting tendency [3].

In the case of experiments denoted as the second batch fig.4a shows that that sudden changes in dimensions recorded in the previous experiments are missing. Slopes during heating represent the coefficient of thermal expansion and the difference between them up to 800°C approximately can be explained by different phase compositions. Samples sintered at 900°C during reheating show a clear phase transition of $ZnTiO_3$ to Zn_2TiO_4 at 951°C. This phase transition on the compacted specimen on fig.1 during sintering occurred at 963°C. The

_____

phase transition is somewhat promoted if heating is performed on a polycrystalline sample. The only detectable influence of the atmosphere change from air to nitrogen is noted in the change in the shrinkage rate shown in fig.4.b. On the onset of shrinkage of samples previously sintered at 1100°C, namely, after 900°C shrinkage rates show dichotomy. Nitrogen atmosphere influences a more abrupt onset to shrinkage with a pronounced exponential slope, while in air the shrinkage rate is somewhat irregular. During the isothermal period the shrinkage rate in both atmospheres coincides, which suggests mass transport diffusion by the oxygen vacancies mechanism.
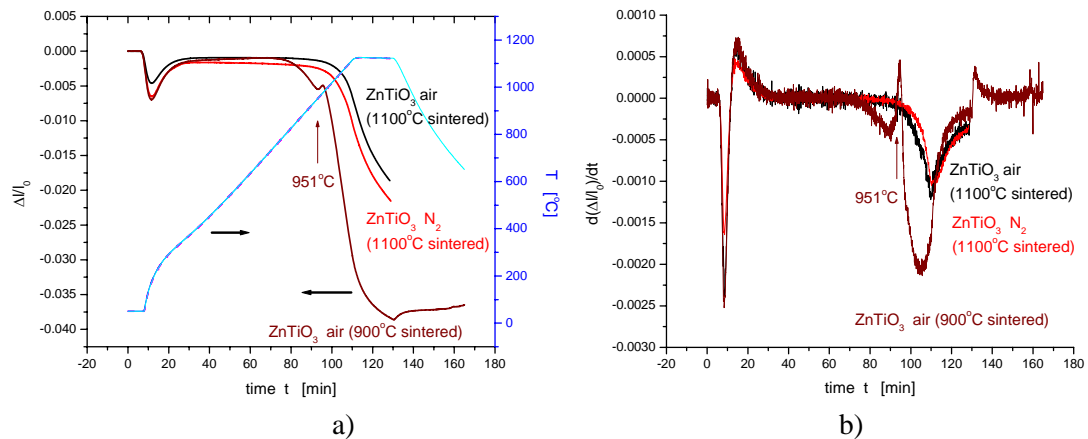

Fig. 4. Second batch of $ZnTiO_3$ specimens, sintered previously at 1100°C and 900°C, reheated up to 1100°C, in air and nitrogen atmosphere; a) dilatation and temperature schedule, and b) shrinkage rate for the same dilatograms.
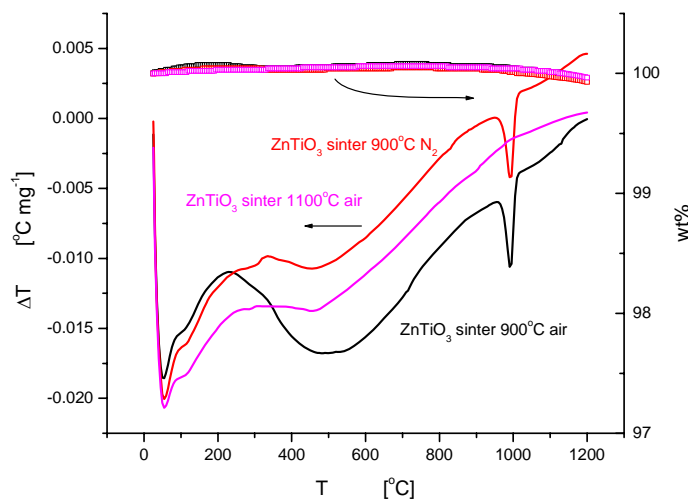

Fig. 5. TGA and DTA function of previously sintered $ZnTiO_3$ at 900°C in nitrogen and air atmosphere and previously sintered at 1200°Cin air atmosphere.

DTA/TGA diagrams recorded for the second batch of sintered specimens are shown in fig. 5. Thermo gravimetric analysis does not show significant changes, leading to the conclusion that interaction of the sintered specimens with atmosphere is negligible. Samples sintered at 1100°C are regarded as completely without a characteristic DTA signal and were recorded only in air atmosphere. They are composed of stable phases, and phase transitions were not expected. Two samples sintered at 900°C, fig.5, show peaks for the $ZnTiO_3$ to Zn_2TiO_4 phase transition. Phase transitions peaks in both atmospheres are positioned at

_____

990°C, which means that the phase transition is not influenced by different atmospheres. There is a difference between these two curves as a broad exothermic peak is visible at around 500°C. It exists only in air atmosphere. This event can be subscribed to favorable air atmosphere for $Zn_2Ti_3O_8$ formation, a low temperature titanate phase [4].

Fig. 6 shows TGA and DTA diagrams obtained for $ZnTiO_3$ nanopowders. The thermo gravimetric change is now substantially pronounced. Due to their extremely large specific surface area values nanopowders are prone to the influence of atmosphere change. At 120°C desorption processes are over and further reduction can be regarded as an interaction of the oxide with the surrounding atmosphere. Both curves, for nitrogen and for air atmosphere, show these weight changes during heating. Different behavior is present after 500°C where the nitrogen atmosphere inhibits mass loss. Interaction with atmosphere is even more enhanced as visible fast mass loss after the $ZnTiO_3$ to Zn_2TiO_4 phase transition. The spinel structure includes cations that exchange places, where transition from inverse to normal spinel can occur [2].

The DTA curve shows a broad peak observed at 500°C that is subscribed to $Zn_2Ti_3O_8$ disappearance and at about 950°C, representing the phase transition from meta $ZnTiO_3$ to orto Zn_2TiO_4. This $Zn_2Ti_3O_8$ disappearance characteristic peak temperature in nitrogen atmosphere is about 80°C lower than in air. The higher temperature phase transition from meta $ZnTiO_3$ to orto Zn_2TiO_4 in this DTA diagram in nitrogen atmosphere is at higher temperature for about 30°C than in air. This shows that for nanopowders more energy is needed in nitrogen atmosphere, probably due to the fact that the vacancies diffusion mechanism is hindered.

Besides the atmosphere influence, in this DTA diagram obtained for the nanopowder the detected meta-orto transition peaks temperatures in both atmospheres are now positioned at lower temperatures than for polycrystalline sintered samples shown in fig.5. Nanopowder particle assemblies are structurally prone to relaxing metastability by phase transition to the ortotitanate form, than in the case of polycrystalline samples formed by previous heating and in such a manner can be regarded as deactivated. This change is visible by comparing the dilatometrical phase transition presented in fig.4, where the onset temperature is at 951°C.
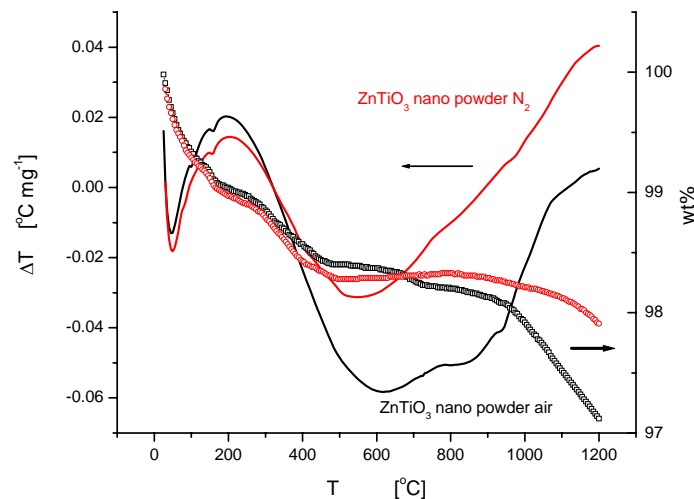

Fig. 6. TGA and DTA function of the $ZnTiO_3$ nanopowder in nitrogen and air atmosphere.

Microstructures of the second batch show the difference between primary sintered samples in air atmosphere, fig.7, and samples reheated in different atmospheres, figs.8 and 9. The grain size determined from the micrograph shown in fig. 7 was estimated as 0.39 microns. The microstructure was recorded on sample breakage, but the grains are rounded and individual grains are pronounced. Grain growth was noted for samples reheated in air atmosphere, fig.8. Reheating in air enlarged grains to the mean value of 0.54 microns. Also,

_____

particular grains are vastly enlarged, and their shape indicates Ostwald ripening grain coalescence. Yet, the main difference occurred between reheated samples in nitrogen atmosphere compared to all other samples obtained in air atmosphere. Namely, samples reheated in nitrogen atmosphere, presented on fig.9, show breakage where the grain boundary is hardly visible and numerous closed pores are present. Closed pores present on the micrographies in fig.9 have a planar polygonal shape with rounded corners and they became visible after breakage at room temperature. The shape of closed pores indicates that they are positioned at grain boundaries triple junctions. Grain growth is concurrent to pore growth and not many closed pores in fig.9 have a circular shape formed by unpinning from the grain boundary. During breaking fast fracture is obtained by crack propagation through the grains. Propagation is further enhanced by stress concentration formed inside the grain close to the pore position. Thus, the pore structure here represents stress concentration sites. Mostly assuming distances between grain boundaries, the grain size can be rudely estimated to 1 micron in diameter. Closed pores in fig.9 can also be measured by the intercept method and their mean size is estimated as 0.32 microns.
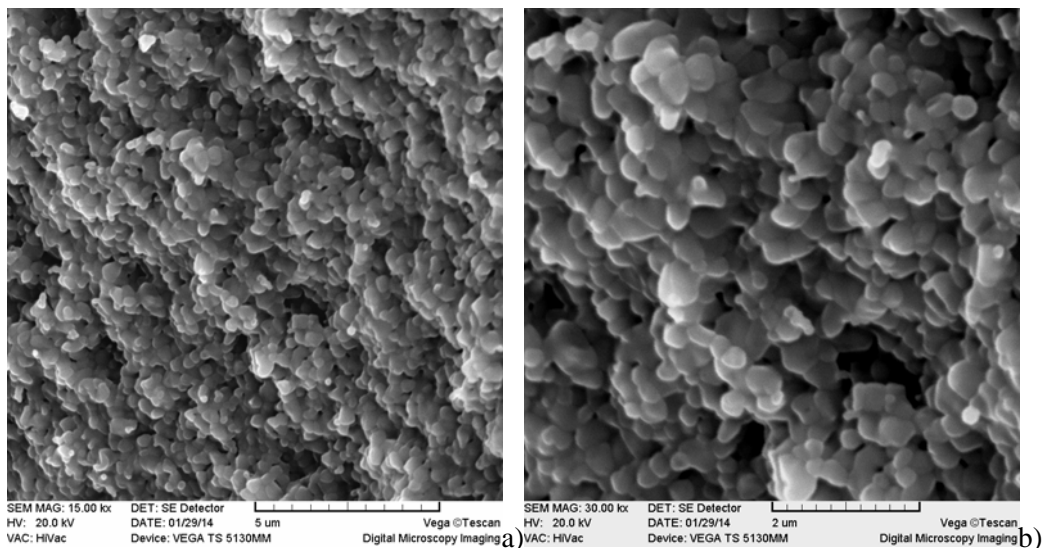

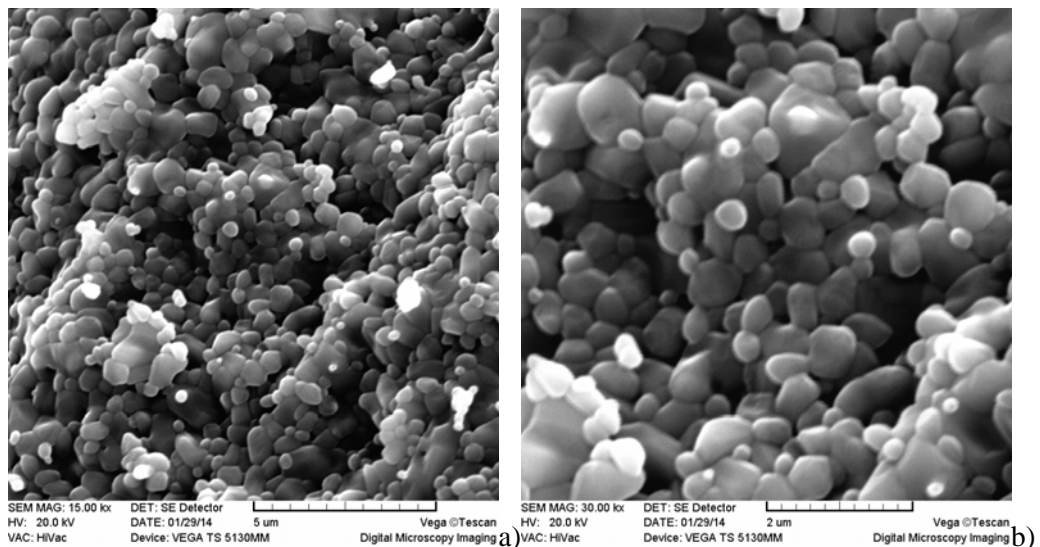**Fig. 7.** $ZnTiO_3$ sintered 1100^oC, 1h, a) 15 kx b) 30 kx enlargement.

Fig. 8. $ZnTiO_3$ reheated 1100^oC, 20 minutes, air atmosphere a) 15 kx b)30 kx enlargement.
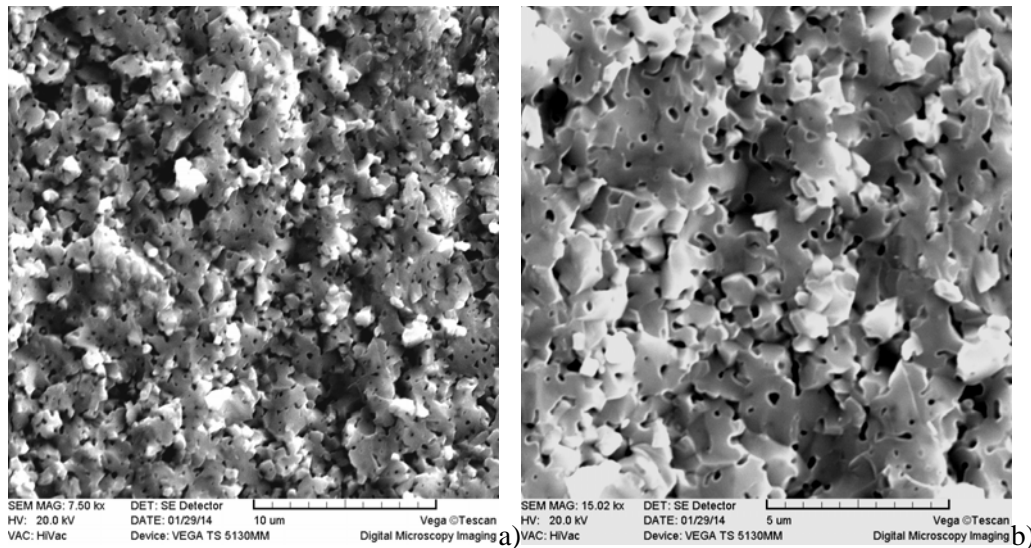
Fig. 9. $ZnTiO_3$ reheated 1100°C, 20 minutes, nitrogen atmosphere, a) 15 kx b)30 kx enlargement.

Microstructures presented here are the most obvious indicator of the difference between microstructures obtained by heating in nitrogen and air atmospheres. Different factors can be the cause of specific microstructure differences: predominant point defects change [19], possible complex changes at the grain boundary [20], point defect annihilation at the surface of the specimen [21], partial pressures differences between pores and atmospheres [22], strain induced by thermal treatment [23], atmosphere solubility [24], previous mechanical treatment [25,26]. Comparing differences just for the first batch and second batch micrographs, all heated in air, we can say that the grain size is different between the first and second batch. Since synthesis routes are not the same this is expected. The supposed main mechanism in oxide structures is usually diffusion enabled by oxygen vacancies migration. Significant TGA mass change recorded for the nanopowder, where the high surface area emphasizes atmosphere differences, shows that oxygen atmosphere compared to a nitrogen atmosphere leads to more intensive mass loss. At the same time in bulk samples TGA analysis show no significant mass loss, while the volume difference recorded on a dilatometric device between oxygen and nitrogen atmospheres is negligible, although different coefficients of thermal expansion can be noted. Nevertheless, grain growth in nitrogen atmosphere was further enhanced, with at the same time extremely pronounced closed pores positioned between grains.

This indicates that vacancies are sustained in the system, and that grain growth is not a subsequent process since it mostly does not unpin pores during grain growth. Vacancies are presumably present in a larger number than in oxygen atmosphere, thus enhancing crystallization. During cooling pores are trapped in sinks at triple junction positions between grains. Stress during cooling is accumulated at the pore-grain-grain boundary junction leading to the before mentioned intergranular cleavage fracture propagation.

4. Conclusion

After nanopowder sintering at 1100°C, subsequent reheating at a higher temperature in air resulted in a grain size of 2.78 microns, which is about 30%, growth. Sintering at lower temperature (900°C) increased grain size during reheating for 34%, up to 0.45 microns. Reheating moved the phase composition towards more stable structures. Reheating sintered polycrystalline samples in nitrogen atmosphere showed no particular changes in dimensions

_____

and heat transfer. Nanopowder sintering exhibited mass loss of about 3% in both atmospheres. Nanopowder sintering showed a phase transition at $500^\circ C$ that lowered the characteristic temperature in nitrogen atmosphere for about $80^\circ C$, while the temperature of the meta-orto phase transition at $950^\circ C$ increased for $30^\circ C$. Characteristic micrographs for polycrystalline reheated specimens show entirely different microstructures if they are reheated in air or in nitrogen atmosphere indicating that diffusion is influenced by atmosphere change. Future interests will include detecting interactions between the most dominating defects on the surface with the atmosphere responsible for consequent pore formation in nitrogen atmosphere.

Acknowledgement

5. References

1. J. Yang, J.H. Swisher, The Phase Stability of $Zn_2Ti_3O_8$, Materials Characterization, 37, 153-159 (1996).
2. M.W.Barsoum, Fundamental of Ceramics, IoP publishing, Ltd, 2003, p.66.
3. J.B.Goodenough, J.M.Longo, "Crystallographic and Magnetic Properties of Perovskite and Perovskite Related Compaunds" Landolt-Börnstein, New Series, Group III, vol.4a, Springer-Verlag, Berlin 1970.
4. O.Yamaguchi, M.Morimi, H.Kawabata, K.Shimizu, Formation and Transformation of $ZnTiO_3$, J.Am.Ceram.Soc., 70 [5], C97-C98 (1987).
5. H.-T. Kim, Y. Kim, M. Valant, D. Suvorov, Titanium Incorporation in Zn_2TiO_4 Spinel Ceramics, J.Am.Ceram.Soc., 84 [5] 1081–86 (2001).
6. N. Labus, J. Krstić, S. Marković, D. Vasiljević-Radović, M V. Nikolić, V. Pavlović, $ZnTiO_3$, Ceramic Nanopowder Microstructure Changes During Compaction, Science of Sintering, 45 (2013) 209-221.
7. Paul Shewmon, Diffusion in solids, 2nd ed., Wiley, 2010, p.189.
8. Paolo M. Ossi, Disorderd Materials, 2ed, Springer, 2006.
9. R. Dieckmann, Point defects and transport in non-stoichiometric oxides: solved and unsolved problems, J.Phys.Chem.Solids, Vol. 59, No.4. pp.507-525, 1998.
10. M. Ozawa, Effect of oxygen release on the sintering of fine CeO_2 powder at low temperature, Scripta Materialia, 50 (2004) 61-64.
11. H.-I. Yoo, J.-H. Lee, M. Martin, J. Janek, H.Schmalzried, Experimental evidence of the interference between ionic and electronic flows in an oxide with prevailing electronic conduction, Solid State Ionics, 67 (1994) 317-322.
12. R. Dieckmann, "Cobaltous Oxide Point Defect Structure and Non-Stoichiometry, Electrical Conductivity, Cobalt Tracer Diffusion." Zeitschrift Für Physikalische Chemie, 107, no. 2 (January 1977): 189–210.
13. M.V. Nikolic, N. Labus, M.M. Ristic, Densification rate and phase structure changes during sintering of zinc titanate ceramics, Ceramics International, 35 (2009) 3217–3220.
14. A.C. Larson, R.B. Von Dreele, General Structure Analysis System (GSAS), Los Alamos National Laboratory Report LAUR 86-748 (2004)
15. B. H. Toby, EXPGUI, a graphical user interface for GSAS, J. Appl. Cryst., 34 (2001) 210-213.

_____

16. M. I. Mendelson, Average Grain Size in Polycrystalline Ceramics, Journal of the American Ceramic Society, Vol.52, No.8., 443-446.

17. N. Labus, J. Vujančević, M.V. Nikolić, Microstructure changes caused by thermal etching of sintered $ZnTiO_3$, PHYSICAL CHEMISTRY 2014, 12th International Conference on Fundamental and Applied Aspects of Physical Chemistry, Belgrade, 22-26 September, 2014.

18. $ZnTiO_3$ Pearson's Crystal Data, Database for Inorganic Compounds, Release 2013/14, Pierre Villars and Karin Cenzual (ed.), Dossier of: 1629506., Publ. ASM International.

19. N.M.Tallan, Defect Characterization by Indirect Experimental Techniques, Battelle Institute Materials Science Colloquia, 8th, Columbus and Salt Fork, Ohio, September 17-22, 1973, Edited by Martin S. Seltzer and Robert I. Jaffee, Defects and transport in oxides, Plenum press, NY, 1974, p.239-250.

20. S.J. Dillon, Complexion: A new concept for kinetic engineering in materials science, Acta Materialia, 55 (2007) 6208–6218.

21. M.A. Henderson, Interaction of Molecular Oxygen with the Vacuum-Annealed $TiO_2(110)$ Surface: Molecular and Dissociative Channels, J. Phys. Chem. B, 1999, 103, 5328-5337.

22. T. Matsudaira, The effect of lutetium dopant on oxygen permeability of alumina polycrystals under oxygen potential gradients at ultra-high temperatures, Acta Materialia, 58 (2010) 1544–1553.

23. D.-J. Shu, Interplay between External Strain and Oxygen Vacancies on a Rutile TiO_2 (110) Surface, Physical Review Letters, 101, 116102 (2008).

24. C. Di Valentin, Origin of the different photo activity of N-doped anatase and rutile TiO_2, Physical Review B, 70, 085116 (2004).

25. N. Obradović, N. Labus, T. Srećković, D. Minić, M. M. Ristić, Synthesis and Characterization of Zinc Titanate Nano-crystal Powders Obtained by Mechanical Activation, Science of Sintering, 37 (2005) 123-129.

26. N. Labus, N. Obradović, T. Srećković, V.Mitić, M.M. Ristić, Influence of Mechanical Activation on Synthesis of Zinc Metatitanate, Science of Sintering, 37 (2005) 115-122.

Садржај: Предмет овог рада био је посматрање промена димензија и топлотног трансфера током загревања узорака ZnTiO₃ у атмосферама азота и ваздуха. Интеракција комадног узорка у току загревања са гасном фазом доводи до уочљивих промена. Узорци добијени синтеровањем нанопраха ZnTiO₃ до различитих температура у ваздуху, подвргнути су накнадном процесу загревања. Током загревања криве дилатације и термогравиметрије са истовременом диференцијалном термалном анализом TGA/DTA су снимљене. Поновно загревање је изведено у атмосферама азота и ваздуха. Тако добијени узорци су микроструктурно окарактерисани сканирајућом електронском микроскопијом SEM. Приказане микростурктуре су међусобно упоређиване. Накнадно загревање у различитим атмосферама доводи до интензивне микроструктурне промене. Добијени резултати упућују на могуће узроке који су довели до разлике у микроструктурама.
Кључне речи: дилатометрија, синтеровање.